

Alpha- and beta-diversity statistical analysis

Supplementary table 1. Statistical analysis of the alpha- and beta-diversity results of the bacteriophage RNA-metagenome. Results with a p-value < 0.05 (bolded) were considered significant.

| Pairwise comparison | Alpha-diversity p-value (Shannon index; Wilcoxon) | Beta-diversity Bray-Curtis p-value (PERMANOVA) | Beta-diversity Jaccard p-value (PERMANOVA) |
|--|---|--|--|
| SARS-CoV-2 positive vs SARS-CoV-2 negative | 0.03 | 0.092 | 0.099 |
| NPS vs TS | <0.001 | 0.001 | 0.001 |
| Symptomatic vs asymptomatic | 0.04 | 0.001 | 0.001 |
| NPS-symptomatic-SARS-CoV-2 positive vs NPS-symptomatic SARS-CoV-2 negative | 1.0 | 0.234 | 0.837 |
| NPS-asymptomatic-SARS-CoV-2 positive vs NPS-asymptomatic-SARS-CoV-2 negative | 0.13 | 0.026 | 0.004 |
| TS-symptomatic-SARS-CoV-2 positive vs TS-symptomatic-SARS-CoV-2 negative | 0.15 | 0.205 | 0.183 |

Volcano plot supplementary data

Supplementary table 2. Significant species ($-\text{Log}_{10}(\text{q-val}) > 1.30$) observed between the fold change of NP symptomatic SARS-CoV-2 positive samples and healthy individuals.

| Species | Log2(FC) | -Log10(q-val) |
|---|-------------------|---------------|
| Actinomyces sp. 2129 | -6.97144210727746 | 3.47998854 |
| Candidatus Saccharibacteria oral taxon TM7x | -6.70612742905151 | 3.47998854 |
| Capnocytophaga sputigena | -6.20647138540253 | 3.47998854 |
| Candidatus Saccharibacteria bacterium FS15P | -6.12285647555089 | 3.47998854 |
| Leptotrichia wadei | -6.01519772707412 | 3.47998854 |
| Leptotrichia goodfellowii | -5.93626931836543 | 3.47998854 |
| Alloprevotella sp. E39 | -5.89713095103068 | 3.47998854 |
| Porphyromonas asaccharolytica | -5.89509017851958 | 3.47998854 |
| Prevotella enoeca | -5.81960075432376 | 3.47998854 |
| Leptotrichia sp. oral taxon 498 | -5.7940315689528 | 3.45070333 |
| Prevotella denticola | -5.50533596550729 | 3.45070333 |
| Atopobium parvulum | -5.48981202698121 | 3.45070333 |
| Candidatus Saccharibacteria bacterium FS13P | -5.47825129694856 | 3.45070333 |
| Actinomyces pacaensis | -5.47309776555904 | 3.45070333 |
| Mogibacterium pumilum | -5.40907989582476 | 3.45070333 |
| [Eubacterium] sulci | -5.39034312529511 | 3.45070333 |
| Candidatus Saccharibacteria bacterium FS07P-B | -5.37981554857233 | 3.45070333 |
| Leptotrichia buccalis | -5.36076216960278 | 3.45070333 |
| Megasphaera stantonii | -5.31276388012429 | 3.45070333 |
| Lachnoanaerobaculum umeaense | -5.30335557184688 | 3.45070333 |
| Leptotrichia shahii | -5.17914229781393 | 3.45070333 |
| Capnocytophaga sp. oral taxon 878 | -5.06660334152056 | 3.45070333 |
| Capnocytophaga leadbetteri | -4.96340744073626 | 3.45070333 |
| Leptotrichia trevisanii | -4.93655421336354 | 3.45070333 |
| Dialister pneumosintes | -4.8398654489815 | 3.45070333 |
| Actinomyces sp. oral taxon 897 | -4.83410605378407 | 3.45070333 |
| Leptotrichia hofstadii | -4.82527976942094 | 3.45070333 |
| Actinomyces hongkongensis | -4.72794972108188 | 3.45070333 |
| Capnocytophaga sp. FDAARGOS_737 | -4.65369071299944 | 3.45070333 |
| Campylobacter showae | -4.63530883523954 | 3.45070333 |
| Porphyromonas gingivalis | -4.62375197991705 | 3.45070333 |
| Leptotrichia hongkongensis | -4.58238675976895 | 3.45070333 |
| Aggregatibacter aphrophilus | -4.53213693250872 | 3.45070333 |
| Capnocytophaga gingivalis | -4.48788660695844 | 3.45070333 |
| Eikenella corrodens | -4.34099040431785 | 3.45070333 |
| Aggregatibacter segnis | -4.24504452131846 | 3.45070333 |
| Haemophilus haemolyticus | -4.23630293732862 | 3.45070333 |
| Haemophilus sp. oral taxon 036 | -4.22416433368701 | 3.45070333 |
| Leptotrichia sp. oral taxon 212 | -4.189810328986 | 3.45070333 |
| Corynebacterium humireducens | -4.18030164571718 | 3.45070333 |

| | | |
|--|-------------------|------------|
| Negativicoccus massiliensis | -4.12262000013304 | 3.45070333 |
| Actinomyces oris | -4.11710346674153 | 3.45070333 |
| Neisseria mucosa | -3.9252969563647 | 3.45070333 |
| Gemella sanguinis | -3.92138823389469 | 3.45070333 |
| Fusobacterium pseudoperiodonticum | -3.81196581078016 | 3.45070333 |
| Olsenella sp. oral taxon 807 | -3.78998872182911 | 3.45070333 |
| Actinomyces sp. oral taxon 171 | -3.70889848452512 | 3.45070333 |
| Haemophilus influenzae | -3.67686400441652 | 3.45070333 |
| Actinomyces naeslundii | -3.60719659993851 | 3.45070333 |
| Corynebacterium matruchotii | -3.59421327644431 | 3.45070333 |
| Haemophilus pittmaniae | -3.49585557798169 | 3.45070333 |
| Haemophilus parahaemolyticus | -3.47624720237673 | 3.45070333 |
| Alloscardovia omnicolens | -3.4307289303342 | 3.45070333 |
| Haemophilus parainfluenzae | -3.36979730047764 | 3.45070333 |
| Fusobacterium periodonticum | -3.3051714153176 | 3.45070333 |
| Bifidobacterium dentium | -3.00693821636284 | 3.45070333 |
| Neisseria sp. oral taxon 014 | -2.94823280134082 | 3.45070333 |
| Campylobacter concisus | -2.94556716439363 | 3.45070333 |
| Actinomyces sp. oral taxon 414 | -2.93383750402153 | 3.45070333 |
| Granulicatella adiacens | -2.8686569181649 | 3.45070333 |
| Neisseria lactamica | -2.84158860704017 | 3.45070333 |
| Fusobacterium hwasookii | -2.80380460694096 | 3.45070333 |
| Actinomyces sp. oral clone CT068 | -2.78396446766446 | 3.45070333 |
| Aggregatibacter actinomycetemcomitans | -2.77224148824293 | 3.45070333 |
| Parvimonas micra | -2.69489722456799 | 3.45070333 |
| Gemella sp. oral taxon 928 | -2.65637290312393 | 3.45070333 |
| Fusobacterium sp. oral taxon 203 | -2.53235950440809 | 3.45070333 |
| Filifactor alocis | -2.50890200329412 | 3.45070333 |
| Capnocytophaga sp. oral taxon 864 | -2.48776724065971 | 3.45070333 |
| Capnocytophaga sp. oral taxon 323 | -2.4778318073797 | 3.45070333 |
| Fusobacterium nucleatum | -2.45795937294954 | 3.45070333 |
| Corynebacterium halotolerans | -2.441696196398 | 3.45070333 |
| Neisseria elongata | -2.4188334385725 | 3.45070333 |
| Capnocytophaga ochracea | -2.3215423094064 | 3.45070333 |
| Bacillus thuringiensis | -2.29592270844087 | 3.45070333 |
| Neisseria subflava | -2.28596703441463 | 3.45070333 |
| Gemella haemolysans | -2.24755234193987 | 3.45070333 |
| Lachnospiraceae bacterium oral taxon 500 | -2.15853712970997 | 3.45070333 |
| Neisseria gonorrhoeae | -2.06050512339854 | 3.45070333 |
| Corynebacterium diphtheriae | -2.00106178768252 | 3.45070333 |
| Neisseria flavescens | -1.80823738467065 | 3.45070333 |
| Human betaherpesvirus 6 | -1.80490481741298 | 3.45070333 |
| Neisseria meningitidis | -1.8009469867746 | 3.45070333 |
| Neisseria sp. KEM232 | -1.78108492075284 | 3.45070333 |
| Neisseria cinerea | -1.7649705373982 | 3.45070333 |

| | | |
|---|-------------------|------------|
| <i>Neisseria polysaccharea</i> | -1.66622862010011 | 3.45070333 |
| <i>Gemella morbillorum</i> | -1.55323460703936 | 3.45070333 |
| <i>Aegilops speltoides</i> | 1.50078402030824 | 3.45070333 |
| <i>Glycine max</i> | 1.78454801936221 | 3.45070333 |
| <i>Glycine soja</i> | 2.04315593520215 | 3.45070333 |
| <i>Enterococcus cecorum</i> | 2.49327327268974 | 3.45070333 |
| <i>Dolosigranulum pigrum</i> | 2.79252744332395 | 3.45070333 |
| <i>Lactobacillus salivarius</i> | 2.99209715348235 | 3.45070333 |
| <i>Lactobacillus paragasseri</i> | 4.27005726906089 | 3.45070333 |
| <i>Lactobacillus paracasei</i> | 5.74866119892748 | 3.45070333 |
| <i>Avena strigosa</i> | 6.31759207050652 | 3.45070333 |
| <i>Lactobacillus vaginalis</i> | 6.42251451263149 | 3.45070333 |
| <i>Lactobacillus rhamnosus</i> | 7.28567106447585 | 3.45070333 |
| <i>Lactobacillus oris</i> | 10.418901156597 | 3.45070333 |
| <i>Prevotella fusca</i> | -6.01450612023137 | 3.45070333 |
| <i>Prevotella intermedia</i> | -5.79960585781393 | 3.36598985 |
| <i>Prevotella melaninogenica</i> | -5.66543034017694 | 3.36598985 |
| <i>Prevotella oris</i> | -5.18490026160827 | 3.36598985 |
| <i>Prevotella jejuni</i> | -5.1027936804828 | 3.28378411 |
| <i>Prevotella histicola</i> | -4.20566144989985 | 3.28378411 |
| <i>Prevotella</i> sp. oral taxon 299 | -7.20121828198195 | 3.28378411 |
| <i>Prevotella ruminicola</i> | -7.03578702715013 | 3.28378411 |
| <i>Selenomonas</i> sp. oral taxon 126 | -5.46049435351101 | 3.28378411 |
| <i>Prevotella scopos</i> | -5.19419967811139 | 3.20862397 |
| <i>Schaalia meyeri</i> | -4.84306784526561 | 3.20862397 |
| <i>Schaalia odontolytica</i> | -4.82068464851997 | 3.20862397 |
| <i>Schaalia cardiffensis</i> | -4.48695028793937 | 3.20862397 |
| <i>Rothia</i> sp. T40-1 | -3.76618528784962 | 3.20862397 |
| <i>Rothia aeria</i> | -3.38828123098386 | 3.20862397 |
| <i>Rothia mucilaginosa</i> | -3.37875110709189 | 3.20862397 |
| <i>Rothia dentocariosa</i> | -1.78692023970928 | 3.20862397 |
| <i>Prevotella salivae</i> | -1.66609396593095 | 3.20862397 |
| <i>Selenomonas</i> sp. oral taxon 920 | -5.79854969244087 | 3.20862397 |
| <i>Selenomonas</i> sp. oral taxon 478 | -4.26232637194894 | 3.17604374 |
| <i>Selenomonas</i> sp. oral taxon 136 | -4.11342541778317 | 3.17604374 |
| <i>Streptococcus</i> phage Javan374 | -6.37430435091126 | 3.17604374 |
| <i>Streptococcus</i> phage Javan371 | -5.16074806832283 | 3.17604374 |
| <i>Streptococcus constellatus</i> | -4.8667877416922 | 3.17604374 |
| <i>Streptococcus</i> phage Javan377 | -4.81163045579993 | 3.17604374 |
| <i>Streptococcus salivarius</i> | -4.74344122456246 | 3.17604374 |
| <i>Streptococcus gordonii</i> | -4.69100139335862 | 3.17604374 |
| <i>Streptococcus</i> sp. oral taxon 064 | -4.39189734686127 | 3.17604374 |
| <i>Streptococcus</i> sp. NPS 308 | -4.23854962978665 | 3.15935379 |
| <i>Streptococcus parasanguinis</i> | -4.07628808657897 | 3.13919268 |
| <i>Streptococcus</i> sp. LPB0220 | -4.07065136900468 | 3.13919268 |

| | | |
|--|-------------------|------------|
| Streptococcus satellite phage Javan323 | -4.0529065871514 | 3.13919268 |
| Streptococcus sp. I-P16 | -3.92212515150516 | 3.13919268 |
| Streptococcus oralis | -3.85588275783764 | 3.13919268 |
| Streptococcus phage Javan355 | -3.81698171293315 | 3.13919268 |
| Streptococcus sp. 1643 | -3.59043277083971 | 3.13919268 |
| Streptococcus infantis | -3.50596874740594 | 3.13919268 |
| Streptococcus sanguinis | -3.29314418106152 | 3.13919268 |
| Streptococcus mitis | -3.20951971793425 | 3.13919268 |
| Streptococcus sp. I-G2 | -3.19734270810211 | 3.13919268 |
| Streptococcus sp. 116-D4 | -3.18109881165719 | 3.13919268 |
| Streptococcus gwangjuense | -3.17934482144221 | 3.13919268 |
| Streptococcus pseudopneumoniae | -3.11662134607058 | 3.13919268 |
| Streptococcus koreensis | -3.11538009387299 | 3.13919268 |
| Streptococcus sp. A12 | -2.99240379301716 | 3.13919268 |
| Streptococcus phage Javan311 | -2.92761284939209 | 3.13919268 |
| Streptococcus pneumoniae | -2.83985801084027 | 3.13919268 |
| Streptococcus intermedius | -2.76795687594035 | 3.13919268 |
| Streptococcus sp. FDAARGOS_192 | -2.62809911571559 | 3.13919268 |
| Streptococcus phage Javan326 | -2.54978052312163 | 3.13919268 |
| Streptococcus australis | -2.44482742924891 | 3.13919268 |
| Selenomonas sputigena | -2.37953002114023 | 3.13919268 |
| Streptococcus equinus | -2.27490843840369 | 3.13919268 |
| Streptococcus satellite phage Javan243 | -1.84368420573697 | 3.13919268 |
| Streptococcus phage Javan310 | -1.78991594155303 | 3.13919268 |
| Streptococcus cristatus | -1.7013210668819 | 3.13919268 |
| Streptococcus sp. oral taxon 431 | -4.84442952288394 | 3.13919268 |
| Streptococcus sp. VT 162 | -3.96391417038777 | 3.13919268 |
| Tannerella sp. oral taxon HOT-286 | -7.02076273899266 | 3.00348563 |
| TM7 phylum sp. oral taxon 488 | -5.61034091656462 | 3.00348563 |
| Veillonella atypica | -5.2218856279505 | 3.00348563 |
| uncultured Caudovirales phage | -5.17515896676709 | 3.00348563 |
| Veillonella dispar | -3.98178798939368 | 3.00348563 |
| Treponema sp. OMZ 804 | -3.87827554075787 | 3.00348563 |
| Veillonella parvula | -3.77690799585285 | 3.00348563 |
| Thermoanaerobacterium xylanolyticum | -3.55987741870961 | 2.83115019 |
| Treponema sp. OMZ 838 | -3.40335858416535 | 2.83115019 |
| Streptococcus virus MS1 | -2.86157337236359 | 2.83115019 |
| Tannerella forsythia | -2.82334586270996 | 2.83115019 |
| Treponema denticola | -2.50603417804985 | 2.47553193 |
| Streptococcus viridans | -2.08487238000787 | 2.47553193 |
| Treponema putidum | -1.51569049179469 | 2.47553193 |

Supplementary table 3. Putative respiratory pathogens identified amongst the NPS samples in COVID-19 positive and COVID-19 negative patients. The proportion of identified organisms were compared using the Fisher's exact test with Benjamini-Hochberg correction.

| Organism | TS | | | P | q-val |
|-----------------------------------|---------------|----------------------|----------------------|--------|-------|
| | All (n=24) | COVID-19 + (n=12) | COVID-19 – (n=12) | | |
| <i>Dolosigranulum pigrum</i> | 12.5% (3/24) | 0% (0/12) | 25% (3/12) | 0.217 | 0.951 |
| <i>Enterobacter</i> | | | | | |
| <i>Enterobacter asburiae</i> | | | | | |
| <i>Enterobacter cloacae</i> | | | | | |
| <i>Enterobacter hormaechei</i> | | | | | |
| <i>Enterobacter ludwigii</i> | 12.5% (3/24) | 16.7% (2/12) | 8.3% (1/12) | >0.999 | 1 |
| <i>Enterobacter sichuanensis</i> | | | | | |
| <i>Enterobacter</i> sp. R4-368 | | | | | |
| <i>Enterobacter roggenkampii</i> | | | | | |
| <i>Haemophilus influenzae</i> | 37.5% (9/24) | 41.7% (5/12) | 33.3% (4/12) | >0.999 | 1 |
| <i>Haemophilus parainfluenzae</i> | 79.2% (19/24) | 66.6% (8/12) | 91.7% (11/12) | 0.317 | 0.951 |
| <i>Klebsiella pneumoniae</i> | 41.7% (10/24) | 16.7% (2/12) | 66.6% (8/12) | 0.008 | 0.072 |
| <i>Serratia marcescens</i> | 4.2% (1/24) | 0% (0/12) | 8.3% (1/12) | >0.999 | 1 |
| <i>Staphylococcus aureus</i> | 25% (6/24) | 16.7% (2/12) | 33.3% (4/12) | 0.640 | 1 |
| <i>Streptococcus pneumoniae</i> | 95.8% (23/24) | 91.7% (11/12) | 100% (12/12) | >0.999 | 1 |
| <i>Streptococcus pyogenes</i> | 4.2% (1/24) | 0% (0/12) | 8.3% (1/12) | >0.999 | 1 |

Supplementary table 4. Putative respiratory pathogens identified amongst the TS samples in COVID-19 positive and COVID-19 negative patients. The proportion of identified organisms were compared using the Fisher's exact test with Benjamini-Hochberg correction.

| Organism | NPS | | | P | q-val |
|-----------------------------------|---------------|----------------------|----------------------|--------|--------------|
| | All (n=47) | COVID-19 + (n=27) | COVID-19 – (n=20) | | |
| <i>Burkholderia multivorans</i> | 17.2% (8/47) | 11.1% (3/27) | 25.0% (5/20) | 0.258 | 0.401 |
| <i>Chlamydia pneumoniae</i> | 2.1% (1/47) | 0% (0/27) | 2.0% (1/20) | 0.069 | 0.322 |
| <i>Dolosigranulum pigrum</i> | 23.4% (11/47) | 40.7% (11/27) | 0% (0/20) | 0.001 | 0.014 |
| <i>Haemophilus influenzae</i> | 4.2% (2/47) | 0% (0/27) | 10.0% (2/20) | 0.196 | 0.372 |
| <i>Haemophilus parainfluenzae</i> | 14.9% (7/47) | 25.9% (7/27) | 0% (0/20) | 0.015 | 0.105 |
| HHV-6 | 2.1% (1/47) | 3.7% (1/27) | 0% (0/20) | >0.999 | 1 |
| Human coronavirus HKU1 | 4.2% (2/47) | 0% (0/27) | 10% (2/20) | 0.175 | 0.372 |
| Human coronavirus NL63 | 2.1% (1/47) | 0% (0/27) | 5.0% (1/20) | 0.425 | 0.507 |
| Influenza A virus | 2.1% (1/47) | 0% (0/27) | 5.0% (1/20) | 0.435 | 0.507 |
| <i>Klebsiella pneumoniae</i> | 2.1% (1/47) | 3.7% (1/27) | 0% (0/20) | >0.999 | 1 |
| <i>Moraxella catharralis</i> | 8.5% (4/47) | 14.8% (4/27) | 0% (0/20) | 0.126 | 0.372 |
| <i>Mycoplasma pneumoniae</i> | 4.3% (2/47) | 0% (0/27) | 10% (2/20) | 0.176 | 0.372 |
| Rhinovirus A | 2.1% (1/47) | 0% (0/27) | 5.0% (1/20) | 0.435 | 0.507 |
| <i>Streptococcus pneumoniae</i> | 14.9% (7/47) | 22.22% (6/27) | 5.0% (1/20) | 0.213 | 0.372 |

Genomic variants supplementary data

Supplementary table 5. SARS-CoV-2 SNPs among the NPS and TS clinical samples, along with its gene, and unique identified features.

| SNP | SNP frequency | Mutation type | Gene/Protein | Unique characteristics and/or predicted changes from wild type | References |
|---------|---------------|-----------------------|--------------|---|------------|
| C100T | 1/274 | N/A | 5'UTR | SNP associated with the P.2 (also known as B.1.1.28.2) Brazilian lineage. | [1] |
| A187G | 6/274 | N/A | 5'UTR | Unresolved. | [2–4] |
| C241T | 20/274 | N/A | 5'UTR | <i>In silico</i> prediction of a weaker interaction of mutant with the MADP1 host-transcription factor [5]. | [5–10] |
| C379A | 3/274 | Synonymous: L64L | ORF1ab/Nsp1 | Unresolved. | [11–14] |
| 507-del | 1/274 | Deletion | ORF1ab/Nsp1 | Unresolved. | Not found. |
| C913T | 1/274 | Synonymous: S36S | ORF1ab/Nsp2 | Associated SNP with the VOC B.1.1.7 | [15] |
| C1059T | 12/274 | Non-synonymous: T266I | ORF1ab/Nsp2 | Unresolved. | [9,16,17] |
| C1616T | 6/274 | Non-synonymous: L271F | ORF1ab/Nsp2 | Unresolved. | Not found |
| C2110T | 1/274 | Synonymous: N435N | ORF1ab/Nsp2 | Unresolved | Not found |
| C2416T | 1/274 | Synonymous: Y537Y | ORF1ab/Nsp2 | Unresolved. | [6] |
| T2423C | 1/274 | Non-synonymous: C540R | ORF1ab/Nsp2 | Unresolved. | Not found |
| G2424A | 2/274 | Non-synonymous: C540Y | ORF1ab/Nsp2 | Unresolved. | Not found |
| A2480G | 1/274 | Non-synonymous: I559V | ORF1ab/Nsp2 | Unresolved. | [13,18,19] |
| G2528A | 1/274 | Non-synonymous: E575K | ORF1ab/Nsp2 | Unresolved. | Not found. |
| C2558T | 1/274 | Non-synonymous: P585S | ORF1ab/Nsp2 | Unresolved. | [13,20–22] |
| C3037T | 21/274 | Synonymous: F106F | ORF1ab/Nsp3 | Unresolved. | 3,12,,13 |
| C3096T | 1/274 | Non-synonymous: S126L | ORF1ab/Nsp3 | Unresolved. | [25,26] |
| C3267T | 1/274 | Non-synonymous: T183I | ORF1ab/Nsp3 | Unresolved | [27] |
| A3405G | 1/274 | Non-synonymous: E229G | ORF1ab/Nsp3 | Unresolved. | Not found. |

| | | | | | |
|---------|-------|---------------------------|------------------------------|---|---------------|
| T3477C | 1/274 | Non-synonymous: V253A | ORF1ab/Nsp3 | Unresolved | Not found |
| T3766C | 1/274 | Synonymous: D349D | ORF1ab/Nsp3 | Unresolved | [28] |
| T3905G | 1/274 | Non-synonymous: F396V | ORF1ab/Nsp3 | Unresolved | Not found. |
| C4534T | 1/274 | Non-synonymous: Y605H | ORF1ab/Nsp3 | Unresolved. | [29] |
| C5144T | 2/274 | Synonymous: L809L | ORF1ab/Nsp3 | Unresolved. | Not found |
| C5694T | 1/274 | Non-synonymous: P992L | ORF1ab/Nsp3 | Unresolved. | [30] |
| C5986T | 1/274 | Synonymous: F1089F | ORF1ab/Nsp3 | Unresolved | [31] |
| G5992T | 1/274 | Non-synonymous: E1091D | ORF1ab/Nsp3 | Unresolved. | Not found |
| C6310T | 2/274 | Synonymous: S1197S | ORF1ab/Nsp3 (NAR domain) | Unresolved. | [13,25] |
| A6425G | 1/274 | Non-synonymous: N1236D | ORF1ab/Nsp3 | Unresolved. | Not found |
| C6664G | 1/274 | Synonymous: V1315V | ORF1ab/Nsp3 | Unresolved. | Not found. |
| A6796G | 1/274 | Synonymous: L1359L | ORF1ab/Nsp3 | Unresolved. | [30] |
| G7675T | 2/274 | Synonymous: A1652A | ORF1ab/Nsp3 | Unresolved. | Not found. |
| G7745A | 1/274 | Non-synonymous: V1676I | ORF1ab/Nsp3 | Unresolved. | Not found. |
| G8083A | 1/274 | Non-synonymous: M1788I | ORF1ab/Nsp3 | Unresolved. | [32] |
| G8216A | 1/274 | Non-synonymous: V1833I | ORF1ab/Nsp3 | Unresolved. | Not found |
| C9438T | 1/274 | Non-synonymous: T295I | ORF1ab/Nsp4 | Unresolved. | [2,33,34] |
| C9711T | 1/274 | Non-synonymous: S387F | ORF1ab/Nsp4 | Unresolved. | [30] |
| C10029T | 1/274 | Non-synonymous: T492I | ORF1ab/Nsp4 | Unresolved. Often referred to as T3255I[35]. Potential signature mutation in the B.1 sub-clade[35]. | [35] |
| C10319T | 2/274 | Non-synonymous: L89F | ORF1ab/3C-like proteinase | Unresolved. | [19,30,36–38] |
| C10422T | 1/274 | Non-synonymous: S123F | ORF1ab/3C-like proteinase | Unresolved. | Not found. |
| C10507T | 1/274 | Synonymous: N151N | ORF1ab/3C-like proteinase | Unresolved. | Not found. |
| T10667G | 1/274 | Non-synonymous: L205V | ORF1ab/3C-like proteinase | SNP associated with the B.1.1.28 Brazilian VOC[28,39] | [28,39] |
| A10770G | 1/274 | Non-synonymous: Y239C | ORF1ab/3C-like proteinase | Unresolved. | [30,37] |
| T11059G | 2/274 | Synonymous: T29T | ORF1ab/Nsp6 | Unresolved. | Not found. |

| | | | | | |
|---------|--------|-----------------------|-----------------------------|--|---------------------|
| G11083T | 1/274 | Non-synonymous: L37F | ORF1ab/Nsp6 | Unresolved. | [13,19,20,22,40,41] |
| C11289T | 1/274 | Non-synonymous: S106F | ORF1ab/Nsp6 | Unresolved. | [30] |
| C11494T | 1/274 | Synonymous: N174N | ORF1ab/Nsp6 | Unresolved. | Not found. |
| C11812A | 1/274 | Synonymous: G280G | ORF1ab/Nsp6 | Unresolved. | Not found. |
| C11824T | 1/274 | Synonymous: I284I | ORF1ab/Nsp6 | Associated SNP with the VOC B.1.1.28 Brazilian clade [42]. | [42,43] |
| C11916T | 1/274 | Non-synonymous: S25L | ORF1ab/Nsp7 | Unresolved. | [13,19,36] |
| C12053T | 2/274 | Non-synonymous: L71F | ORF1ab/Nsp7 | Linked to increased severity outcome[44]. Odds ratio of 17.80 associated with increased death among Brazilian patients. Linked to G25088T (S: V11176F) SNP[45]. | [44,45] |
| C12357T | 1/274 | Non-synonymous: T89I | ORF1ab/Nsp8 | Unresolved. | [30,46] |
| C12412T | 1/274 | Synonymous: I107I | ORF1ab/Nsp8 | Unresolved. | [30,47] |
| C12789T | 1/274 | Non-synonymous: T35I | ORF1ab/Nsp9 | Unresolved. | [30] |
| G12794A | 1/274 | Non-synonymous: G37R | ORF1ab/Nsp9 | Unresolved. | Not found. |
| A12964G | 1/274 | Synonymous: G93G | ORF1ab/Nsp9 | SNP associated with the P.2 (also known as B.1.1.28.2) Brazilian lineage[1]. | [1,48] |
| C13335T | 1/274 | Non-synonymous: A104V | ORF1ab/Nsp10 | Unresolved. | [30] |
| T14313C | 1/274 | Synonymous: D291D | ORF1ab/RdRp | Unresolved. | [30] |
| C14408T | 23/274 | Non-synonymous: P323L | ORF1ab/RdRp | Unresolved modified activity. This mutant are more likely to have mutations in the membrane (M) and envelope proteins (E)[49]. Suggested to rigidify the RdRp protein structure[49]. | [6,9,23,49–52] |
| G14559T | 1/274 | Synonymous: V373V | ORF1ab/RdRp | Unresolved. | Not found. |
| C14805T | 1/274 | Synonymous: Y455Y | ORF1ab/RdRp | Typically found with G11083T and G26114T[53] | [8,9,53] |
| T16176C | 1/274 | Synonymous: T912T | ORF1ab/RdRp | Unresolved. | [31] |
| C16806T | 2/274 | Synonymous: N190N | ORF1ab/Helicase | Unresolved. | [30] |
| G17014T | 4/274 | Non-synonymous: D260Y | ORF1ab/Helicase | Unresolved. | [46] |
| A17066G | 1/274 | Non-synonymous: Y277C | ORF1ab/Helicase | Unresolved | Not found. |
| G18155A | 1/274 | Non-synonymous: C39Y | ORF1ab/3' to 5' exonuclease | Unresolved. | Not found. |
| A18424G | 1/274 | Non-synonymous: N129D | ORF1ab/3' to 5' exonuclease | Unresolved. | [32] |
| G18651T | 1/274 | Non-synonymous: E204D | ORF1ab/3' to 5' exonuclease | Unresolved | Not found |
| C18998T | 1/274 | Non-synonymous: A320V | ORF1ab/3' to 5' exonuclease | Unresolved. | [13,45,54] |
| A19578G | 2/274 | Synonymous: Q513Q | ORF1ab/3' to 5' exonuclease | Unresolved. | Not found. |
| A19974G | 1/274 | Synonymous: P118P | ORF1b/EndoRNAse | Unresolved. | [30] |
| C19983T | 1/274 | Synonymous: V121V | ORF1b/EndoRNAse | Unresolved. | [55] |
| G20014T | 2/274 | Non-synonymous: D132Y | ORF1b/EndoRNAse | Unresolved. | Not found |

| | | | | | |
|---------|--------|------------------------|-------------------------------|---|---------------------|
| C20480T | 1/274 | Non-synonymous: S288L | ORF1b/EndoRNase | Unresolved. | Not found |
| G21088T | 1/274 | Non-synonymous: D144Y | ORF1ab/2'-O-methyltransferase | Unresolved. | [30] |
| C21302T | 1/274 | Non-synonymous P215L | ORF1ab/2'-O-methyltransferase | Unresolved. | [30] |
| C21304A | 1/274 | Non-synonymous: R216S | ORF1ab/2'-O-methyltransferase | Unresolved. | [23,30] |
| G21305A | 1/274 | Non-synonymous: R216H | ORF1ab/2'-O-methyltransferase | Unresolved. | [30] |
| C21306T | 1/274 | Synonymous: R216R | ORF1ab/2'-O-methyltransferase | Unresolved. | [30] |
| A21583G | 1/274 | Synonymous: L7L | S/Surface glycoprotein | Unresolved. | Not found |
| G23012A | 1/274 | Non-synonymous: E484K | S/Surface glycoprotein | Confers resistance to monoclonal antibodies[56]. Mutant associated with the P.1 (Brazil) and B.1.351 (South Africa) VOC[57].May improve binding affinity between RBD and the hACE2 receptor, potentially increasing transmission . Associated with cases of re-infection in Brazilian patients ^{57,59} . | 45,56–59 |
| A23064C | 1/274 | Non-synonymous: N501T | S/Surface glycoprotein | This mutant could potentially increase the binding affinity between SARS-CoV-2 and the human receptor ACE2 ^{60–64} . | 60–65 |
| C23271A | 1/274 | Non-synonymous: A570T | S/Surface glycoprotein | SNP associated with the B.1.1.7 VOC ⁶⁶ . Mutant correlated with 70% more transmissibility than the wild type ⁴⁵ . | 45,66,67 |
| A23403G | 19/274 | Non-synonymous: D614G | S/Surface glycoprotein | Unresolved modified activity. Found simultaneously with G25563T variation on ORF3a ⁹ . Potentially increased infectivity* ^{68,69} | 4,8,9,23,24,68,69 |
| G23608T | 2/274 | Synonymous: R682R | S/Surface glycoprotein | Unresolved. | Not found. |
| A23756G | 1/274 | Non-synonymous: T732A | S/Surface glycoprotein | Unresolved. | 30 |
| G25088T | 1/274 | Non-synonymous: V1176F | S/Surface glycoprotein | Correlated to increased mortality in Brazilian and Saudi-Arabian patients. Typically present with the D614G mutant ⁷⁰ . | 70 |
| A25097G | 1/274 | Non-synonymous: I1179V | S/Surface glycoprotein | Unresolved. | Not found. |
| G25234T | 1/274 | Non-synonymous: L1224F | S/Surface glycoprotein | Unresolved. | 71 |
| G25563T | 17/274 | Non-synonymous: Q57H | ORF3a/ORF3a protein | Unresolved modified activity. Typically found in C27964T mutants ⁷² . | 9,13,30,47,50,72–74 |
| C25603T | 1/274 | Synonymous: L71L | ORF3a/ORF3a protein | Unresolved. | Not found. |
| C25688T | 1/274 | Non-synonymous: A99V | ORF3a/ORF3a protein | Unresolved. | 26 |
| A25718G | 1/274 | Non-synonymous: Y109C | OR3a/ORF3a protein | Unresolved. | 75 |
| C27213T | 1/274 | Synonymous: L4L | ORF6/ORF6 protein | Unresolved. | 26 |
| C27964T | 7/274 | Non-synonymous: S24L | ORF8/ORF8 protein | Unresolved modified activity. Typically found in G25563T mutants ⁷² . | 13,30,72,76,77 |
| C27972T | 1/274 | Nonsense: Q27Stop | ORF8/ORF8 protein | Truncates the ORF8 protein and potentially inactivates the protein. This variant has been associated with the B.1.1.7 VOC ³¹ | 15,31,78 |
| G28048T | 1/274 | Non-synonymous: R52I | ORF8/ORF8 protein | SNP associated with the B.1.1.7 VOC ^{15,31,79} . | 15,31,79 |
| A28095T | 1/274 | Nonsense: K68Stop | ORF8/ORF8 protein | This mutant has been found to be present along with the Q27Stop mutation ⁸⁰ . | 80 |
| A28111G | 1/274 | Non-synonymous: Y73C | ORF8/ORF8 protein | SNP typically found in B.1.1.7 VOC ⁸¹ . | 81,82 |
| C28253T | 1/274 | Synonymous: F120F | ORF8/ORF8 protein | Unresolved. | 29,83 |

| | | | | | |
|---------|-------|-----------------------|-------------------------------|---|------------|
| 28270 Δ | 1/274 | Deletion | N/A | Unresolved. | 30,84 |
| C28472T | 1/274 | Non-synonymous: P67S | N/Nucleocapsid phosphoprotein | Unresolved. | 30,32 |
| G28628T | 1/274 | Non-synonymous: A119S | N/Nucleocapsid phosphoprotein | SNP associated with the P.2 (also known as B.1.1.28.2) Brazilian lineage ¹ . | 1,39 |
| C28869T | 1/274 | Non-synonymous: P199L | N/Nucleocapsid phosphoprotein | Unresolved. | 85 |
| G28881A | 2/274 | Non-synonymous: R203K | N/Nucleocapsid phosphoprotein | *Unknown function. SNPs G28881A, G28882A, G28883C typically found together in a homopolymer mutant. Strong allelic pairwise association of the three SNPs clustered together. | 7,8,74,86 |
| G28882A | 2/274 | Non-synonymous: R203K | N/Nucleocapsid phosphoprotein | *Unknown function. SNPs G28881A, G28882A, G28883C typically found together in a homopolymer mutant. Strong allelic pairwise association of the three SNPs clustered together. | 7,8,86 |
| G28883C | 2/274 | Non-synonymous: G204R | N/Nucleocapsid phosphoprotein | *Unknown function. SNPs G28881A, G28882A, G28883C typically found together in a homopolymer mutant. Strong allelic pairwise association of the three SNPs clustered together. | 7,8,86 |
| T28921C | 6/274 | Synonymous: D206D | N/Nucleocapsid phosphoprotein | Unresolved. | Not found. |
| G28975T | 6/274 | Non-synonymous: M234I | N/Nucleocapsid phosphoprotein | Unresolved. | 85 |
| C28977T | 6/274 | Non-synonymous: S235F | N/Nucleocapsid phosphoprotein | Characteristic mutation of the B.1.1.7 VOC. ⁸¹ Predicted to provide a stabilization effect to the N protein. ⁸² | 15,81,82 |
| A29412T | 1/274 | Non-synonymous: Q380L | N/Nucleocapsid phosphoprotein | Unresolved. | Not found. |
| G29540A | 1/274 | Non-translatable SNP | 3'UTR | Unresolved. | 87,88 |
| 29743Δ | 1/274 | Deletion | 3'UTR | Unresolved. | Not found |
| 29746Δ | 1/274 | Deletion | 3'UTR | Unresolved. | 89 |
| 29749Δ | 1/274 | Deletion | 3'UTR | Unresolved. | 90 |
| C29754T | 1/274 | Non-translatable SNP | 3'UTR | SNP associated with the P.2 (also known as B.1.1.28.2) Brazilian lineage ¹ . | 1 |
| C29835T | 1/274 | Non-translatable SNP | 3'UTR | Unresolved. | Not found. |

Supplementary table 6. Identified SNPs per patient with its correspondent mutant, lineage and method used for lineage identification. Highlighted SNPs have been previously correlated to VOC/VOIs.

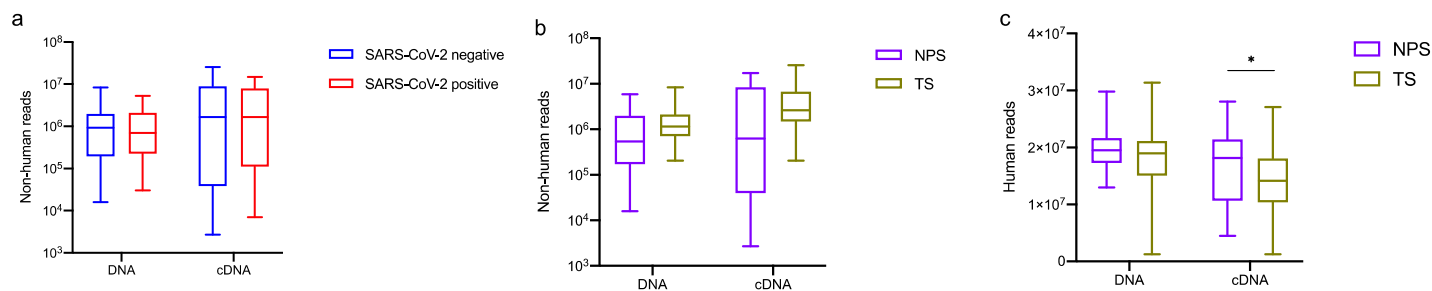
| Patient ID | Identified SNPs | Identified mutants | VOC lineage |
|------------|--|--|-------------|
| P004 | C241T, C379A, C1059T, C3037T, C14408T, G25563T | Nsp1: L64L Nsp2: T266I; Nsp3: F106F; RdRp: P323L; ORF3a protein: Q57H | N/A |
| P019 | C241T, C1059T, C3037T, G8216A, C14408T, G18155A, A23403G, G25563T | Nsp2: T266I; Nsp3: F106F; V1833I; RdRp: P323L; 3' to 5' exonuclease: C39Y; Surface glycoprotein: D614G; ORF3a protein: Q57H | N/A |
| P022 | C241T, C1059T, C3037T, C14408T, G17014T, A23403G, G25563T, C27964T | Nsp2: T266I; Nsp3: F106F; RdRp: P323L; Helicase: D260Y; Surface glycoprotein: D614G; ORF3a protein: Q57H; ORF8 protein: S24L | N/A |
| P35 | A187G, C241T, C1616T, C3037T, C14408G, A17066G, C19983T, A23403G | Nsp2: L271F; Nsp3: F106F; RdRp: P323L; Helicase: Y277C; EndoRNase: V121V; Surface glycoprotein: D614G | N/A |
| P066 | A187G, C241T, C1616T, C3037T, C14408T | Nsp2: L271F; Nsp3: F106F; RdRp: P323L | N/A |
| P069 | A187G, C241T, C1616T, C3037T, C14408T, A23403G, G23608T, A25097G | Nsp2: L271F; Nsp3: F106F; RdRp: P323L; Surface glycoprotein: D614G, R682R, I1179V | N/A |
| P082 | C241T, C1059T, C3037T, C14408T, A23403G, G25563T, C25688T | Nsp2: T266I; Nsp3: F106F; RdRp: P323L; Surface glycoprotein: D614G; ORF3a protein: Q57H, A99V | N/A |
| P721 | C241T, C1059T, C3037T, C6664G, A6796G, G8083A, C10319T, C12357T, C14408T, C14805T, A18424G, G21088T, C21302T, C21304A, G21305A, A23403G, G25563T, C27964T, C28472T, C28869T, A29412T | Nsp2: T266I; Nsp3: F106F, V1315V, L1359L, M1788I; 3C-like proteinase: L89F; Nsp8: T89I; RdRp: P323L, Y455Y; 3' to 5' exonuclease: N129D; 2-O-methyltransferase: 216H, P215L, R216S, R216H; Surface glycoprotein: D614G; ORF3a protein: Q57H; ORF8 protein: S24L; Nucleocapsid phosphoprotein: P67S, P199L, Q380L | N/A |
| P259 | C1059T, C3037T, A23403G, G25563T | Nsp2: T266I; Nsp3: F106F; Surface glycoprotein: D614G; ORF3a protein: Q57H | N/A |
| P725 | C1059T, C3037T, A23403G, G25563T | Nsp2: T266I; Nsp3: F106F; Surface glycoprotein: | N/A |

| | | | |
|--------|---|--|----------------------------|
| | | D614G; ORF3a protein: Q57H | |
| P264 | C241T, C1059T, T2423C, C3037T, C3096T, C5144T, C14408T, G17014T, A23403G, G25563T, C27964T | Nsp2: T266I, C540R; Nsp3: F106F, S126L, L809L; RdRp: P323L; Helicase: D260Y; Surface glycoprotein: D614G; ORF3a protein: Q57H; ORF8 protein: S24L | N/A |
| P267 | C3037T, C4534T, C5144T, C14408T, G17014T, A23403G, G25563T, C27964T | Nsp3: F106F, Y605H, L809L; RdRp: P323L; Helicase: D260Y; Surface glycoprotein: D614G; ORF3a protein: Q57H; ORF8 protein: S24L | N/A |
| P273 | C241T, C1059T, C3037T, T3905G, C6310T, A10770G, T11059G, C14408T, A23064C, G23608T, G25563T, C27964T | Nsp2: T266I; Nsp3: F106F, F396V, S1197S, 3C-like proteinase: Y239C; Nsp6: T29T; RdRp: P323L; Surface glycoprotein: N501T, R682R; ORF3a protein: Q57H; ORF8 protein: S24L | N/A |
| P276 | C241T, 507del, C1059T, C3037T, G5992T, C10422T, T11059G, C14408T, G17014T, A23403G, G25563T, C27964T | Nsp2: T266I; Nsp3: F106F, E1091D; 3C-like proteinase: S123F; Nsp6: T29T; RdRp: P323L; Helicase: D260Y; Surface glycoprotein: D614G; ORF3a protein: Q57H; ORF8 protein: S24L | N/A |
| P281 | C241T, C3037T, C12412T, T14313C, C14408T, A23403G, G28881A, G28882A, G28883C | Nsp3: F106F; Nsp8: I107I; RdRp: D291D, P323 (or P314L in NSP12b)L; Surface glycoprotein: D614G; Nucleocapsid phosphoprotein: R203K, G204R | Potentially VOC P.2 |
| P289 | A2480G, C2558T, C6310T, G11083T, C13335T | Nsp2: I559V, P585S; Nsp3: S1197S; Nsp6:L37F; Nsp10: A104V | N/A |
| P297 | C241T, C379A, C1059T, C3037T, C14408T, C20480T, A23403G, G25563T | Nsp1: L64L Nsp2: T266I; Nsp3: F106F; RdRp: P323L; EndoRNase: S288L; Surface glycoprotein: D614G; ORF3a protein: Q57H | N/A |
| P303 | C241T, C379A, C1059T, C3037T, C14408T, G25563T | Nsp1: L64L Nsp2: T266I; Nsp3: F106F; RdRp: P323L; ORF3a protein: Q57H | N/A |
| P306 | A187G, C241T, C1616T, C3037T, A6425G, G7675T, C9348T, C14408T, A23403G | Nsp2: L271F; Nsp3: F106F, N1236, A1652A; Nsp4: T295I; RdRp: P323L; Surface glycoprotein: D614G | N/A |
| P311 | A187G, C241T, C1616T, C3037T, A23403G | Nsp2: L271F; Nsp3: F106F; Surface glycoprotein: D614G | N/A |
| P312 | A187G, C241T, C1616T, C3037T, G7675T, C14408T | Nsp2: L271F; Nsp3: F106F, A1652A; RdRp: P323L | N/A |
| P733 | C10319T, C10507T, C11289T, A23403G, G25563T, C27964T, C28472T, C28869T | 3C-like proteinase: L89F, N151N; Nsp6: S106F; Surface glycoprotein: D614G; ORF3a protein: Q57H; ORF8 protein: S24L; Nucleocapsid phosphoprotein: P67S, P199L | N/A |
| P344 | C241T, A23403G, G25563T | Surface glycoprotein: D614G; ORF3a protein: Q57H | N/A |
| P348 | C241T, C2416T, G2528A, A3405G, C11494T, C14408T, C16806T, G18651T, G20014T, A23403G, G25234T, G25563T, A25718G, C27213T, 29743del | Nsp2: Y537Y, E575K; Nsp3: E229G; Nsp6: N174N; RdRp: P323L; Helicase: N190N; 3' to 5' exonuclease: E204D; EndoRNase: D132Y; Surface glycoprotein: D614; L1224F; ORF3a protein: Q57H, Y109C; ORF6 protein: L4L | N/A |
| P734 | C10029T, C12789T, G12794A, G14559T, A19974G, C21306T, A23756G, G28881A, G28882A, G28883C, T28912C | Nsp4: T492I; Nsp9: T35I; Nsp9: G37R; RdRp: V373V; EndoRNase: P118P; 2-O-methyltransferase: R216R; Surface glycoprotein: T732A; Nucleocapsid phosphoprotein: R203K, G204R, D260D | N/A |
| P356 | C11812A, C16806T, G20014T | Nsp6: G280G; Helicase: N190N; EndoRNase: D132Y | N/A |
| P363 | C11916T, C14408T, C18998T, A21583G, G25563T, G29540A, 29746del, 29749del | Nsp7: S25L; RdRp: P323L; 3' to 5' exonuclease: A320V; Surface glycoprotein: L7L; ORF3a protein: Q57H | N/A |
| P369 | C14408T, G28881A, G28882A, G28883C | RdRp: P323L; Nucleocapsid phosphoprotein: R203K, G204R | N/A |
| P739** | C913T, C2110T, C3267T, C5986T, G7745A, C14408T, T16176C, C23271A, C25603T, C27972T, G28048T, A28095T, A28111G | Nsp2: S36S, N435N; Nsp3: T183I, A890D, F1089F, I1412T, V1676I; Nsp6: 104-107 del; RdRp: P323L (or P314L in NSP12b), T912T; Surface glycoprotein: 69/70 del, 144 del, N501Y, A570D, P681H, D1118H; ORF3a protein: L71L; ORF8 protein: Q27Stop, R52I, K68Stop, Y73C; Nucleocapsid phosphoprotein: 3DL, S253F | B.1.1.7 United Kingdom VOC |
| P743 | G2424A, C12053T, C14408T, A19578G, G28628T, G28881A, G28882A, G28883C, C29754T | Nsp2: C540Y Nsp7: L71F; RdRp: P323L (or P314L in NSP12b); 3' to 5' exonuclease: Q513Q; Nucleocapsid phosphoprotein: A119S, R203K, G204R | P.2 Brazilian VOC |
| P744 | C100T, C241T, G2424A, C3037T, T3477C, T3766C, C5694T, C9711T, T10667G, C11824T, C12053T, A12964G, C14408T, A19578G, G23012A, A23403G, G25088T, C28253T, G28628T, G28881A, G28882A, G28883C, G28975T, C29754T, C29835T | 5'UTR: R81C, Nsp2: C540Y; Nsp3: F106F, V253A, D349D, P992L; Nsp4: S387F; 3C-like proteinase: L205V; Nsp6: I284I; Nsp7: L71F; Nsp9: G93G; RdRp: P323L (or P314L in NSP12b); 3' to 5' exonuclease: Q513Q; Surface glycoprotein: E484K, D614G, V1176F; ORF8 protein: F120F; Nucleocapsid phosphoprotein: A119S, R203K, G204R, M234I | P.2 Brazilian VOC |

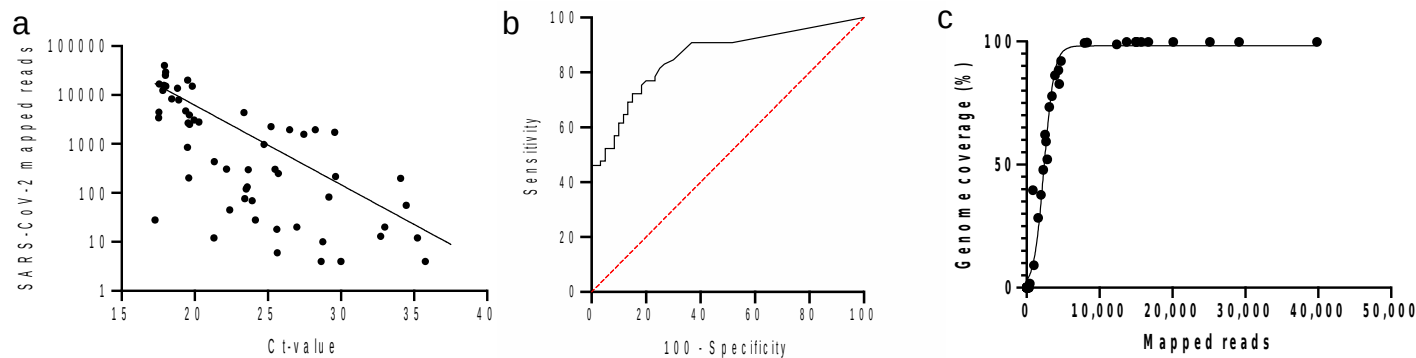
*: Homopolymer stretch of three SNPs occur in the two codons, the G2881A and G28882A translate together to lysine (K).

**: Majority of SNPs were detected under the default parameter threshold for SNP calling from IDseq.

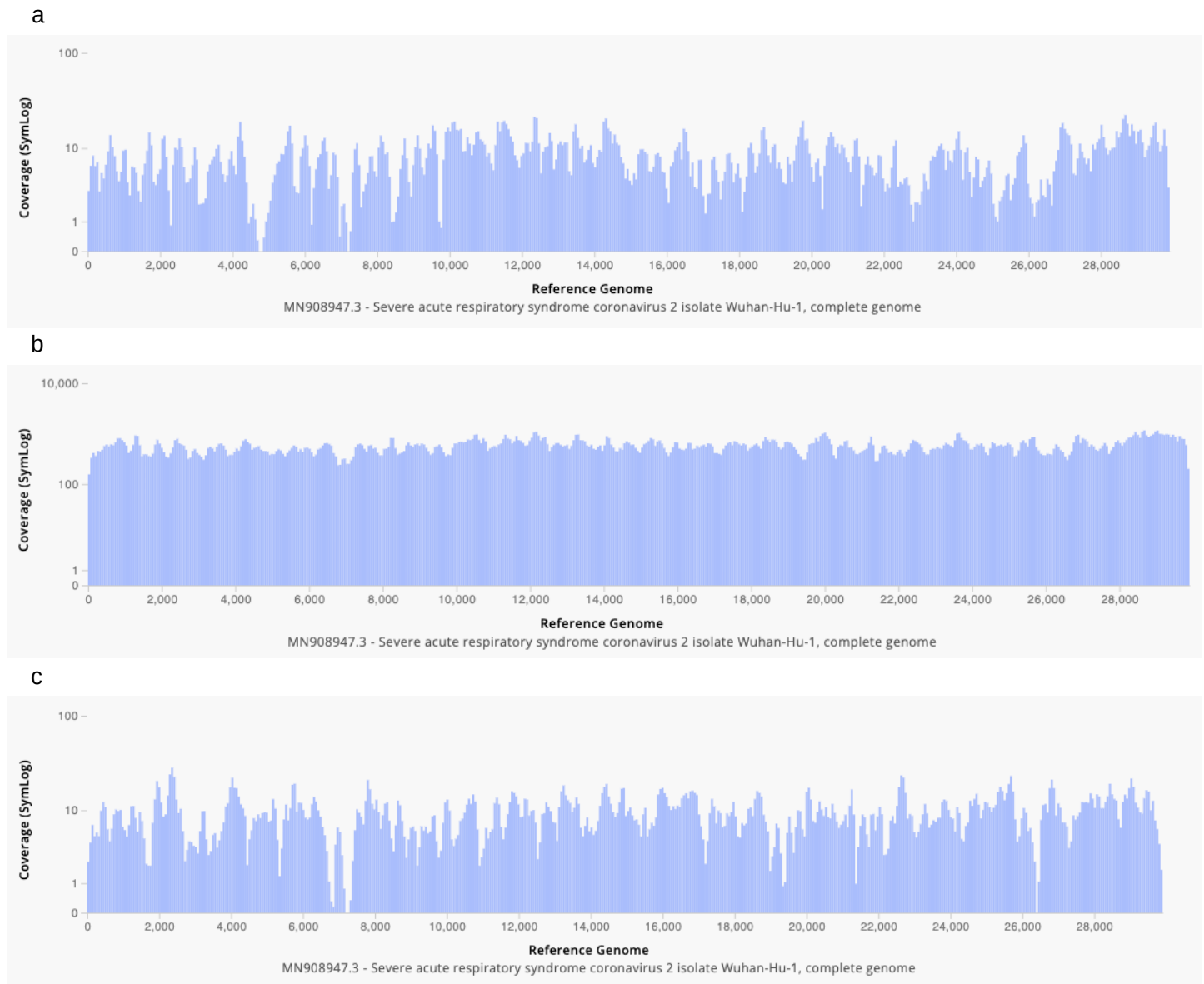
Supplementary figures



Supplementary figure 1. Number of human and non-human DNA and cDNA reads between SARS-CoV-2 diagnosis and anatomical swabbing site. (a) Number of non-human DNA and cDNA reads by SARS-CoV-2 diagnosis. Number of non-human (b) and human (c) DNA and cDNA reads by anatomical swabbing site. (*) indicates a significant p-value below 0.05.



Supplementary figure 2. Regression analysis and ROC evaluation of all the clinical samples (n=125). (a) Exponential regression model of SARS-CoV-2 mapped reads vs RT-PCR Ct value. (b) ROC curve evaluation with a red dashed line depicting the 0.50 AUC. (c) Logistic regression model of genome coverage vs number of mapped reads.



Supplementary figure 3. Genome coverage visualization of the (a,b) Zeta VOIs and the (c) Alpha VOC identified. The ‘y’ axis represents the depth of coverage of each nucleotide and the ‘x’ axis represents the nucleotide position of the MN908947.3 reference genome.

References:

1. Ferrareze, P. A. G. *et al.* E484K as an innovative phylogenetic event for viral evolution: Genomic analysis of the E484K spike mutation in SARS-CoV-2 lineages from Brazil. *bioRxiv* 2021.01.27.426895 (2021) doi:10.1101/2021.01.27.426895.
2. Yang, X., Dong, N., Chan, E. W.-C. & Chen, S. Genetic cluster analysis of SARS-CoV-2 and the identification of those responsible for the major outbreaks in various countries. *Emerg. Microbes Infect.* **9**, 1287–1299 (2020).

3. Large scale genomic analysis of 3067 SARS-CoV-2 genomes reveals a clonal geo-distribution and a rich genetic variations of hotspots mutations. 25.
4. Identification of super-transmitters of SARS-CoV-2. 38.
5. Chaudhari, A. *et al.* In-Silico analysis reveals lower transcription efficiency of C241T variant of SARS-CoV-2 with host replication factors MADP1 and HNRNP-1. *bioRxiv* 2020.11.22.393009 (2020) doi:10.1101/2020.11.22.393009.
6. Mercatelli, D. & Giorgi, F. M. Geographic and Genomic Distribution of SARS-CoV-2 Mutations. *Front. Microbiol.* **11**, (2020).
7. Mishra, A. *et al.* Mutation landscape of SARS-CoV-2 reveals three mutually exclusive clusters of leading and trailing single nucleotide substitutions. 19.
8. Yang, H.-C. *et al.* Analysis of genomic distributions of SARS-CoV-2 reveals a dominant strain type with strong allelic associations. *Proc. Natl. Acad. Sci.* **117**, 30679–30686 (2020).
9. UGUREL, O. M., ATA, O. & TURGUT-BALIK, D. An updated analysis of variations in SARS-CoV-2 genome. *Turk. J. Biol.* **44**, 157–167 (2020).
10. Bartolini, B. *et al.* SARS-CoV-2 Phylogenetic Analysis, Lazio Region, Italy, February–March 2020 - Volume 26, Number 8—August 2020 - Emerging Infectious Diseases journal - CDC. doi:10.3201/eid2608.201525.
11. Sashittal, P., Luo, Y., Peng, J. & El-Kebir, M. Characterization of SARS-CoV-2 viral diversity within and across hosts. *bioRxiv* 2020.05.07.083410 (2020) doi:10.1101/2020.05.07.083410.
12. Wan, J. *et al.* Human-IgG-Neutralizing Monoclonal Antibodies Block the SARS-CoV-2 Infection. *Cell Rep.* **32**, 107918 (2020).
13. Gomez-Carballa, A., Bello, X., Pardo-Seco, J., Martinon-Torres, F. & Salas, A. Mapping genome variation of SARS-CoV-2 worldwide highlights the impact of COVID-19 super-spreaders. *Genome Res.* gr.266221.120 (2020) doi:10.1101/gr.266221.120.
14. Guo, L. *et al.* Genomic epidemiology of the Los Angeles COVID-19 outbreak. *medRxiv* 2020.09.15.20194712 (2020) doi:10.1101/2020.09.15.20194712.

15. Public Health England. Investigation of SARS-CoV-2 variants of concern in England.
16. Liu, S. *et al.* Genetic Spectrum and Distinct Evolution Patterns of SARS-CoV-2. *Front. Microbiol.* **11**, (2020).
17. Zhang, W. *et al.* Analysis of SARS-CoV-2 Genomes from Southern California Reveals Community Transmission Pathways in the Early Stage of the US COVID-19 Pandemic.
<http://medrxiv.org/lookup/doi/10.1101/2020.06.12.20129999> (2020) doi:10.1101/2020.06.12.20129999.
18. Lemieux, J. E. *et al.* Phylogenetic analysis of SARS-CoV-2 in Boston highlights the impact of superspreading events. *Science* **371**, (2021).
19. Gámbaro, F. *et al.* Introductions and early spread of SARS-CoV-2 in France, 24 January to 23 March 2020. *Eurosurveillance* **25**, (2020).
20. Hanifehnezhad, A. *et al.* Characterization of local SARS-CoV-2 isolates and pathogenicity in IFNAR^{-/-} mice. *Heliyon* **6**, e05116 (2020).
21. Martin, J. *et al.* Tracking SARS-CoV-2 in Sewage: Evidence of Changes in Virus Variant Predominance during COVID-19 Pandemic. *Viruses* **12**, (2020).
22. Li, J. *et al.* Rapid genomic characterization of SARS-CoV-2 viruses from clinical specimens using nanopore sequencing. *Sci. Rep.* **10**, 17492 (2020).
23. DEMİR, A. B., BENVENUTO, D., ABACIOĞLU, H., ANGELETTI, S. & CICCIOZZI, M. Identification of the nucleotide substitutions in 62 SARS-CoV-2 sequences from Turkey. *Turk. J. Biol.* **44**, 178–184 (2020).
24. Nguyen, T. T. *et al.* Genetic diversity of SARS-CoV-2 and clinical, epidemiological characteristics of COVID-19 patients in Hanoi, Vietnam. *PLOS ONE* **15**, e0242537 (2020).
25. Salazar, C. *et al.* Multiple introductions, regional spread and local differentiation during the first week of COVID-19 epidemic in Montevideo, Uruguay. <http://biorxiv.org/lookup/doi/10.1101/2020.05.09.086223> (2020) doi:10.1101/2020.05.09.086223.
26. Snell, L. B. *et al.* Combined epidemiological and genomic analysis of nosocomial SARS-CoV-2 transmission identifies community social distancing as the dominant intervention reducing outbreaks.
medRxiv 2020.11.17.20232827 (2020) doi:10.1101/2020.11.17.20232827.

27. Loconsole, D. *et al.* Genome Sequence of a SARS-CoV-2 VUI 202012/01 Strain Identified from a Patient Returning from London, England, to the Apulia Region of Italy. *Microbiol. Resour. Announc.* **10**, (2021).
28. Franceschi, V. B. *et al.* Genomic Epidemiology of SARS-CoV-2 in Esteio, Rio Grande do Sul, Brazil. *medRxiv* 2021.01.21.21249906 (2021) doi:10.1101/2021.01.21.21249906.
29. Wen, S. *et al.* High-coverage SARS-CoV-2 genome sequences acquired by target capture sequencing. *J. Med. Virol.* **92**, 2221–2226 (2020).
30. Joshi, M. *et al.* Genomic variations in SARS-CoV-2 genomes from Gujarat: Underlying role of variants in disease epidemiology. *bioRxiv* 2020.07.10.197095 (2020) doi:10.1101/2020.07.10.197095.
31. Preliminary genomic characterisation of an emergent SARS-CoV-2 lineage in the UK defined by a novel set of spike mutations - SARS-CoV-2 coronavirus / nCoV-2019 Genomic Epidemiology. *Virological* <https://virological.org/t/preliminary-genomic-characterisation-of-an-emergent-sars-cov-2-lineage-in-the-uk-defined-by-a-novel-set-of-spike-mutations/563> (2020).
32. Pater, A. A. *et al.* Emergence and Evolution of a Prevalent New SARS-CoV-2 Variant in the United States. *bioRxiv* 2021.01.11.426287 (2021) doi:10.1101/2021.01.11.426287.
33. Leist, S. R. *et al.* A Mouse-Adapted SARS-CoV-2 Induces Acute Lung Injury and Mortality in Standard Laboratory Mice. *Cell* **183**, 1070-1085.e12 (2020).
34. SARS-CoV-2 has observably higher propensity to accept uracil as nucleotide substitution: Prevalence of amino acid substitutions and their predicted functional implications in circulating SARS-CoV-2 in India up to July, 2020 - Abstract - Europe PMC. <https://europepmc.org/article/PPR/PPR223256>.
35. Shen, L. *et al.* Emerging variants of concern in SARS-CoV-2 membrane protein: a highly conserved target with potential pathological and therapeutic implications. *bioRxiv* 2021.03.11.434758 (2021) doi:10.1101/2021.03.11.434758.
36. Zeng, L., Li, D., Tong, W., Shi, T. & Ning, B. Biochemical features and mutations of key proteins in SARS-CoV-2 and their impacts on RNA therapeutics. *Biochem. Pharmacol.* 114424 (2021) doi:10.1016/j.bcp.2021.114424.

37. Gimeno, A. *et al.* Prediction of Novel Inhibitors of the Main Protease (M-pro) of SARS-CoV-2 through Consensus Docking and Drug Reposition. *Int. J. Mol. Sci.* **21**, (2020).
38. Turakhia, Y. *et al.* Stability of SARS-CoV-2 phylogenies. *PLOS Genet.* **16**, e1009175 (2020).
39. Phylogenetic relationship of SARS-CoV-2 sequences from Amazonas with emerging Brazilian variants harboring mutations E484K and N501Y in the Spike protein - SARS-CoV-2 coronavirus / nCoV-2019 Genomic Epidemiology. *Virological* <https://virological.org/t/phylogenetic-relationship-of-sars-cov-2-sequences-from-amazonas-with-emerging-brazilian-variants-harboring-mutations-e484k-and-n501y-in-the-spike-protein/585> (2021).
40. Sekizuka, T. *et al.* Haplotype networks of SARS-CoV-2 infections in the Diamond Princess cruise ship outbreak. *Proc. Natl. Acad. Sci. U. S. A.* **117**, 20198–20201 (2020).
41. Capobianchi, M. R. *et al.* Molecular characterization of SARS-CoV-2 from the first case of COVID-19 in Italy. *Clin. Microbiol. Infect. Off. Publ. Eur. Soc. Clin. Microbiol. Infect. Dis.* **26**, 954–956 (2020).
42. Spike E484K mutation in the first SARS-CoV-2 reinfection case confirmed in Brazil, 2020 - SARS-CoV-2 coronavirus / nCoV-2019 Genomic Epidemiology. *Virological* <https://virological.org/t/spike-e484k-mutation-in-the-first-sars-cov-2-reinfection-case-confirmed-in-brazil-2020/584> (2021).
43. Løvestad, A. H., Jørgensen, S. B., Handal, N., Ambur, O. H. & Aamot, H. V. Investigation of intra-hospital SARS-CoV-2 transmission using nanopore whole genome sequencing. *J. Hosp. Infect.* **0**, (2021).
44. Nagy, Á., Pongor, S. & Györfy, B. Different mutations in SARS-CoV-2 associate with severe and mild outcome. *Int. J. Antimicrob. Agents* **57**, 106272 (2021).
45. Fang, S. *et al.* Updated SARS-CoV-2 Single Nucleotide Variants and Mortality Association. *medRxiv* 2021.01.29.21250757 (2021) doi:10.1101/2021.01.29.21250757.
46. Patro, L. P. P., Sathyaseelan, C., Uttamrao, P. P. & Rathinavelan, T. Global variation in the SARS-CoV-2 proteome reveals the mutational hotspots in the drug and vaccine candidates. *bioRxiv* 2020.07.31.230987 (2020) doi:10.1101/2020.07.31.230987.

47. Gniazdowski, V. *et al.* Repeat COVID-19 Molecular Testing: Correlation of SARS-CoV-2 Culture with Molecular Assays and Cycle Thresholds. *Clin. Infect. Dis. Off. Publ. Infect. Dis. Soc. Am.* (2020) doi:10.1093/cid/ciaa1616.
48. Francisco, R. da S. *et al.* Pervasive transmission of E484K and emergence of VUI-NP13L with evidence of SARS-CoV-2 co-infection events by two different lineages in Rio Grande do Sul, Brazil. *medRxiv* 2021.01.21.21249764 (2021) doi:10.1101/2021.01.21.21249764.
49. Eskier, D., Karakülâh, G., Suner, A. & Oktay, Y. RdRp mutations are associated with SARS-CoV-2 genome evolution. *PeerJ* **8**, (2020).
50. Yuan, F., Wang, L., Fang, Y. & Wang, L. Global SNP analysis of 11,183 SARS-CoV-2 strains reveals high genetic diversity. *Transbound. Emerg. Dis.* (2020) doi:10.1111/tbed.13931.
51. Yu, J.-M. *et al.* Analysis of Continuous Mutation and Evolution on Circulating SARS-CoV-2. *Evol. Bioinforma.* **16**, 1176934320954870 (2020).
52. Pachetti, M. *et al.* Emerging SARS-CoV-2 mutation hot spots include a novel RNA-dependent-RNA polymerase variant. *J. Transl. Med.* **18**, 179 (2020).
53. Kim, J.-M. *et al.* Genomic investigation of the coronavirus disease-2019 outbreak in the Republic of Korea. *Sci. Rep.* **11**, 6009 (2021).
54. Everett, J. *et al.* SARS-CoV-2 Genomic Variation in Space and Time in Hospitalized Patients in Philadelphia. *mBio* **12**, (2021).
55. Velasco, J. M. *et al.* Coding-Complete Genome Sequences of 23 SARS-CoV-2 Samples from the Philippines. *Microbiol. Resour. Announc.* **9**, (2020).
56. Xie, X. *et al.* Neutralization of SARS-CoV-2 spike 69/70 deletion, E484K and N501Y variants by BNT162b2 vaccine-elicited sera. *Nat. Med.* 1–2 (2021) doi:10.1038/s41591-021-01270-4.
57. Nonaka, C. K. V. *et al.* Early Release - Genomic Evidence of SARS-CoV-2 Reinfection Involving E484K Spike Mutation, Brazil - Volume 27, Number 5—May 2021 - Emerging Infectious Diseases journal - CDC. doi:10.3201/eid2705.210191.

58. Wang, W. B. *et al.* E484K mutation in SARS-CoV-2 RBD enhances binding affinity with hACE2 but reduces interactions with neutralizing antibodies and nanobodies: Binding free energy calculation studies. *bioRxiv* 2021.02.17.431566 (2021) doi:10.1101/2021.02.17.431566.
59. Resende, P. C. *et al.* Genomic surveillance of SARS-CoV-2 reveals community transmission of a major lineage during the early pandemic phase in Brazil. *bioRxiv* 2020.06.17.158006 (2020) doi:10.1101/2020.06.17.158006.
60. Wan, Y., Shang, J., Graham, R., Baric, R. S. & Li, F. Receptor Recognition by the Novel Coronavirus from Wuhan: an Analysis Based on Decade-Long Structural Studies of SARS Coronavirus. *J. Virol.* **94**, (2020).
61. Fiorentini, S. *et al.* First detection of SARS-CoV-2 spike protein N501 mutation in Italy in August, 2020. *Lancet Infect. Dis.* **0**, (2021).
62. Ahamad, S., Kanipakam, H. & Gupta, D. Insights into the structural and dynamical changes of spike glycoprotein mutations associated with SARS-CoV-2 host receptor binding. *J. Biomol. Struct. Dyn.* 1–13 doi:10.1080/07391102.2020.1811774.
63. Welkers, M. R. A., Han, A. X., Reusken, C. B. E. M. & Eggink, D. Possible host-adaptation of SARS-CoV-2 due to improved ACE2 receptor binding in mink. *Virus Evol.* **7**, (2021).
64. Sardar, R., Satish, D., Birla, S. & Gupta, D. Integrative analyses of SARS-CoV-2 genomes from different geographical locations reveal unique features potentially consequential to host-virus interaction, pathogenesis and clues for novel therapies. *Heliyon* **6**, e04658 (2020).
65. Shang, J. *et al.* Structural basis of receptor recognition by SARS-CoV-2. *Nature* **581**, 221–224 (2020).
66. Calcagnile, M., Forgez, P., Alifano, M. & Alifano, P. The lethal triad: SARS-CoV-2 Spike, ACE2 and TMPRSS2. Mutations in host and pathogen may affect the course of pandemic. *bioRxiv* 2021.01.12.426365 (2021) doi:10.1101/2021.01.12.426365.
67. Kemp, S. A. *et al.* Recurrent emergence and transmission of a SARS-CoV-2 Spike deletion Δ H69/ Δ V70. *bioRxiv* 2020.12.14.422555 (2020) doi:10.1101/2020.12.14.422555.
68. Korber, B. *et al.* Spike mutation pipeline reveals the emergence of a more transmissible form of SARS-CoV-2. *bioRxiv* 2020.04.29.069054 (2020) doi:10.1101/2020.04.29.069054.

69. Zhang, L. *et al.* The D614G mutation in the SARS-CoV-2 spike protein reduces S1 shedding and increases infectivity. *bioRxiv* 2020.06.12.148726 (2020) doi:10.1101/2020.06.12.148726.
70. Farkas, C., Mella, A. & Haigh, J. J. Large-scale population analysis of SARS-CoV-2 whole genome sequences reveals host-mediated viral evolution with emergence of mutations in the viral Spike protein associated with elevated mortality rates. *medRxiv* 2020.10.23.20218511 (2020) doi:10.1101/2020.10.23.20218511.
71. Long, S. W. *et al.* Molecular Architecture of Early Dissemination and Massive Second Wave of the SARS-CoV-2 Virus in a Major Metropolitan Area. *medRxiv* 2020.09.22.20199125 (2020) doi:10.1101/2020.09.22.20199125.
72. Cai, H. Y., Cai, K. K. & Li, J. Identification of Novel Missense Mutations in a Large Number of Recent SARS-CoV-2 Genome Sequences. *J. Biotechnol. Biomed.* **3**, 93–103 (2020).
73. Hu, Y. & Riley, L. W. Dissemination and co-circulation of SARS-CoV2 subclades exhibiting enhanced transmission associated with increased mortality in Western Europe and the United States. *medRxiv* 2020.07.13.20152959 (2020) doi:10.1101/2020.07.13.20152959.
74. Paul, D. *et al.* Phylogenomic analysis of SARS-CoV-2 genomes from western India reveals unique linked mutations. (2020).
75. Majumdar, P. & Niyogi, S. ORF3a mutation associated with higher mortality rate in SARS-CoV-2 infection. *Epidemiol. Infect.* **148**,.
76. Yu, Y. *et al.* *CovProfile: profiling the viral genome and gene expressions of SARS-COV-2.* <http://biorxiv.org/lookup/doi/10.1101/2020.04.05.026146> (2020) doi:10.1101/2020.04.05.026146.
77. Leuzinger, K. *et al.* Epidemiology and precision of SARS-CoV-2 detection following lockdown and relaxation measures. *J. Med. Virol.* **93**, 2374–2384 (2021).
78. Lopez-Rincon, A. *et al.* Design of Specific Primer Set for Detection of B.1.1.7 SARS-CoV-2 Variant using Deep Learning. *bioRxiv* 2020.12.29.424715 (2020) doi:10.1101/2020.12.29.424715.
79. Tu, H. *et al.* Distinct Patterns of Emergence of SARS-CoV-2 Spike Variants including N501Y in Clinical Samples in Columbus Ohio. *bioRxiv* 2021.01.12.426407 (2021) doi:10.1101/2021.01.12.426407.

80. Pereira, F. SARS-CoV-2 variants combining spike mutations and the absence of ORF8 may be more transmissible and require close monitoring. *Biochem. Biophys. Res. Commun.* **550**, 8–14 (2021).
81. Galloway, S. E. Emergence of SARS-CoV-2 B.1.1.7 Lineage — United States, December 29, 2020–January 12, 2021. *MMWR Morb. Mortal. Wkly. Rep.* **70**, (2021).
82. Singh, J., Ehtesham, N. Z., Rahman, S. A. & Hasnain, S. E. Structure-function investigation of a new VUI-202012/01 SARS-CoV-2 variant. *bioRxiv* 2021.01.01.425028 (2021) doi:10.1101/2021.01.01.425028.
83. Harper, H. *et al.* Detecting SARS-CoV-2 variants with SNP genotyping. *bioRxiv* 2020.11.18.388140 (2020) doi:10.1101/2020.11.18.388140.
84. Khatamzas, E. *et al.* Emergence of multiple SARS-CoV-2 mutations in an immunocompromised host. *medRxiv* 2021.01.10.20248871 (2021) doi:10.1101/2021.01.10.20248871.
85. Ward, D. *et al.* An integrated in silico immuno-genetic analytical platform provides insights into COVID-19 serological and vaccine targets. *Genome Med.* **13**, 4 (2021).
86. Caccuri, F. *et al.* A persistently replicating SARS-CoV-2 variant derived from an asymptomatic individual. *J. Transl. Med.* **18**, 362 (2020).
87. LitCovid. <https://www.ncbi.nlm.nih.gov/research/coronavirus/>.
88. Ryder, S. P., Morgan, B. R. & Massi, F. Analysis of Rapidly Emerging Variants in Structured Regions of the SARS-CoV-2 Genome. *bioRxiv* 2020.05.27.120105 (2020) doi:10.1101/2020.05.27.120105.
89. Miller, D. *et al.* Full genome viral sequences inform patterns of SARS-CoV-2 spread into and within Israel. *Nat. Commun.* **11**, 5518 (2020).
90. Khailany, R. A., Safdar, M. & Ozaslan, M. Genomic characterization of a novel SARS-CoV-2. *Gene Rep.* **19**, 100682 (2020).